Original Article

MOLECULAR METABOLISM

GPSM1 in POMC neurons impairs brown adipose tissue thermogenesis and provokes diet-induced obesity

Mengyang Tang [1,2], Yi Zhang [3], Rong Zhang [3], Yuemei Zhang [3], Jiangfei Zheng [3], Daixi Wang [3], Xinyu Wang [4], Jing Yan [3,], Cheng Hu [1,2,3,*]**

ABSTRACT

Objective: G-protein-signaling modulator 1 (GPSM1) has been proved the potential role in brain tissues, however, whether GPSM1 in hypothalamic nuclei, especially in POMC neurons is essential for the proper regulation of whole-body energy balance remains unknown. The aim of our current study was to explore the role of GPSM1 in POMC neurons in metabolic homeostasis.

Methods: We generated POMC neuron specific *GPSM1* deficiency mice and subjected them to a High Fat Diet to monitor metabolic phenotypes *in vivo*. By using various molecular, biochemical, immunofluorescent, immunohistochemical analyses, and cell culture studies to reveal the pathophysiological role of GPSM1 in POMC neurons and elucidate the underlying mechanisms of GPSM1 regulating POMC neurons activity.

Results: We demonstrated that mice lacking *GPSM1* in POMC neurons were protected against diet-induced obesity, glucose dysregulation, insulin resistance, and hepatic steatosis. Mechanistically, *GPSM1* deficiency in POMC neurons induced enhanced autophagy and improved leptin sensitivity through PI3K/AKT/mTOR signaling, thereby increasing POMC expression and α-MSH production, and concurrently enhancing sympathetic innervation and activity, thus resulting in decreased food intake and increased brown adipose tissue thermogenesis.

Conclusions: Our findings identify a novel function of GPSM1 expressed in POMC neurons in the regulation of whole-body energy balance and metabolic homeostasis by regulating autophagy and leptin sensitivity, which suggests that GPSM1 in the POMC neurons could be a promising therapeutic target to combat obesity and obesity-related metabolic disorders.

Keywords Obesity; Thermogenesis; Autophagy; Leptin sensitivity; GPSM1

1. INTRODUCTION

Obesity, caused by an excessive accumulation of fat in the body [1], is a global health concern and a major risk factor for the development of numerous complications, including type 2 diabetes [2], cardiovascular disease [2,3], kidney and liver disease [4,5], and certain types of cancer [6,7], imposing profound economic and health care burdens on both society and individuals [8]. Obesity is caused by the chronic imbalance between food intake and energy expenditure, both of which are controlled by complex neuronal activities [9–11]. Therefore, a deeper understanding of the neuroregulatory mechanisms underlying obesity might provide new approaches for its treatment.

The central nervous system (CNS), especially the arcuate nucleus (ARC) in the hypothalamus, which could sense and integrate diverse signals reflecting nutritional status, therefore, playing a critical role in controlling energy homeostasis [12–14]. Among the multiple neural populations within the ARC, AgRP neurons that express orexigenic agouti-related protein, and POMC neurons that express anorexigenic neuropeptides cocaine and pro-opiomelanocortin, are most widely studied [15,16]. Previous studies have identified various molecules and pathways, including MANF, ATF4/ATG5, PTP1B, and endoplasmic reticulum stress [17–20], that are important for POMC neurons in maintaining energy balance and metabolic homeostasis. Further elucidating how POMC neurons exert metabolic control is warranted for combating obesity.

G-protein-signaling modulator 1 (GPSM1), also known as activator of G-protein signaling 3, is broadly expressed in various tissues, including brain [21,22]. Researches have provided evidence that GPSM1 participates $G_{\beta\gamma}$-mediated mitotic spindle orientation in cell division of cerebral cortical progenitors [23] and regulates drug or cocaine-seeking behavior in the prefrontal cortex [24]. Hofler and Koelle identified that GPSM1 regulates food seeking behavior in the CNS of

[1]The Third School of Clinical Medicine, Southern Medical University, Guangzhou, China [2]Department of Endocrinology and Metabolism, Fengxian Central Hospital Affiliated to Southern Medical University, Shanghai, China [3]Shanghai Diabetes Institute, Shanghai Key Laboratory of Diabetes Mellitus, Shanghai Clinical Center for Diabetes, Shanghai Sixth People's Hospital Affiliated to Shanghai Jiao Tong University School of Medicine, Shanghai, China [4]School of Life Science and Technology of ShanghaiTech University, Shanghai, China

*Corresponding author.The Third School of Clinical Medicine, Southern Medical University, Guangzhou, China. E-mail: alfredhc@sjtu.edu.cn (C. Hu).

**Corresponding author. E-mail: jingyan_1216@vip.163.com (J. Yan).

Received July 3, 2023 • Revision received November 1, 2023 • Accepted November 14, 2023 • Available online 17 November 2023

https://doi.org/10.1016/j.molmet.2023.101839

Caenorhabditis elegans [25]. Thus, we wonder that whether GPSM1 in CNS, especially hypothalamus, has the vital effect on energy balance and metabolic homeostasis.

In this study, mice with POMC-neuron-specific knockout of *GPSM1* (PGKO) were used to investigate the contribution of GPSM1 to whole-body energy balance. We find that PGKO mice were protected against diet-induced obesity, glucose dysregulation and insulin resistance. Moreover, GPSM1 in POMC neurons was required for the thermogenesis in brown adipose tissue (BAT) by modulating its sympathetic innervation. Mechanistically, *in vivo* and *in vitro* studies demonstrated that GPSM1 in POMC neurons was a novel regulator of autophagy and leptin signaling, both of which are crucial for regulating the activation of POMC neurons.

2. MATERIALS AND METHODS

2.1. Animals and treatments

All mice used in our experiments were C57BL/6J background. C57BL/6J and Rosa26-tdTOMATO (Ai9) mice were purchased from GemPharmatech Co. Ltd. Mice bearing a conditional loxP-flanked allele of *GPSM1* (*GPSM1*$^{f/f}$, LoxP, used as control mice) were generated under the C57BL/6J genetic background by GemPharmatech Co. Ltd, in which exon 2—11 of the GPSM1 allele was flanked by loxP sites. LoxP mice were intercrossed with the POMC-Cre line to create POMC-neuron-specific *GPSM1*-knockout (*GPSM1*^{PKO}, PGKO) mice. For determination of the specificity and efficiency of *GPSM1* deletion, PGKO mice were intercrossed with Ai9 mice to generate PGKO/Ai9 mice, for labeling of the POMC neurons *in vivo*. POMC-Cre mice were kindly provided by professor Ilya A. Vinnikov (College of Life Science and Technology, Shanghai Jiao Tong University).

All animal studies were supervised and approved by the Animal Care Committee of Shanghai Sixth People's Hospital affiliated to Shanghai Jiao Tong University School of Medicine, and the animal welfare ethics acceptance number is No: 2018-0133. Mice were housed under a 12-hour light and 12-hour dark cycle in a temperature-controlled room (22°C—24 °C), with free access to water, normal chow-diet (NCD, P1200F, Shanghai Puluteng Co. Ltd) or high fat-diet (HFD, 60 % fat, D12492, Research Diets). The mice were housed with 3—5 per cage. At the end of the experiment (for DIO (diet induced obesity) mice: HFD for 10—14 weeks; for NCD mice: feeding for 20—22 weeks), mice were euthanized via CO2-dependent asphyxiation and tissues were harvested.

2.2. Metabolic phenotyping

Body weight of all mice was recorded weekly. A rectal thermometer (ThermalertTH-5, Physitemp, USA) was used to measure core temperature at 2p.m. Fat and lean mass were determined by Dual Energy X-ray Absorptiometry (lnAlyzer, Seoul, South Korea). Before measuring oxygen consumption, carbon dioxide production, energy expenditure, food intake and locomotor activity, the mice were first put in an OxyMax Comprehensive Laboratory Animal Monitoring System (Columbus, St Paul, USA) for 24 h for adapting, and then monitored these data for 24 h.

For glucose tolerance tests (GTTs), mice were deprived of food for 6 h and intraperitoneally (i.p.) injected with D-glucose (Millipore) solution at a dose of 1 g/kg (HFD) or 2 g/kg (NCD) body weight. For insulin tolerance tests (ITTs), mice were fasted for 4 h before i.p. injection of 0.75 U/kg (NCD) or 1.25 U/kg (HFD) insulin (Novo Nordisk). Blood glucose levels were measured from the tail vein blood before (0 min) and at 15, 30, 60, 90, 120 min after glucose or insulin injection using a hand-held glucometer (Accu-Chek glucose reader, Roche).

For leptin sensitivity tests, mice were individually housed and i.p. injected with saline for 5 consecutive days for adaption. On the sixth day, mice were fasted for 12 h prior to injection of leptin (5 mg/kg, 498-OB-05M, R&D Systems, USA). Food intake was detected in 1, 4, 8, 12, 24 h after leptin injection. For immunostaining, mice were fasted for 12 h and i.p. injected with leptin (3 mg/kg). 45 min later, mice were rapidly perfused and brains were processed for immunostaining for p-STAT3 or c-FOS.

For cold-stress experiments, 12-week-old mice were placed in a refrigerator (4 °C) for 6 h and monitored rectal temperature at 0, 1, 3, 4, 6 h. For collecting serum and tissues, the mice were placed in the refrigerator (4 °C) for 8 h.

Plasma was collected after fasted for 16 h. Insulin and leptin ELISA kit (90080, 90030, Crystal Chem, USA) were used to quantify plasma insulin and leptin levels. Serum corticosterone levels was measured by a corticosterone ELISA kit (H205-1-2, Nanjing Jiancheng Bioengineering Institute, Nanjing, China). Serum noradrenaline levels was measured by a Noradrenaline high sensitive ELISA kit (BA E-5200R, LDN Germany). Hypothalami from mice were broken and sonicated in 500ul HCl (0.1N) solution. Lysates were centrifuged and supernatants were collected for detecting α-MSH contents using a α-MSH EIA kit (EK-043-01, Phoenix Pharmaceuticals, USA). All biochemical analyses were carried out according to the instructions of manufacturers.

2.3. Fiber photometry

To record *in vivo* calcium transients in POMC neurons in freely moving mice by using a fiber photometry system (R810, RWD, Shenzhen, China), male POMC-Cre or PGKO mice (4 weeks upon an HFD) were anesthetized, and then, on an ultra-precise stereotaxic instrument (RWD), received stereotaxic injections of 400 nl of AAV-EF1α-DIO-GCaMP6s virus (5×10^{12}viral genomes/ml, BrainVTA, Wu Han, China) into the ARC (anteroposterior (AP), −1.50 mm; mediolateral (ML), +0.25 mm; and dorsoventral (DV), −5.90 mm). At the same time, an optical fiber (RWD) was implanted over the ARC (AP, −1.50 mm; ML, +0.25 mm; and DV, −5.70 mm) and fixed to the skull by using dental acrylic. After surgery, all the mice were individually housed to recovery for 3 weeks upon an HFD.

Before formal experiment, mice were habituated to daily handing and i.p. saline injections for 5 consecutive days to minimize external stimulus that may alter calcium signal. Each mouse was recorded for 10 min baseline and 30 min after i.p. injections of leptin (5 mg/kg). All the experiments were performed between 9 am and 12 pm. The light intensity at the tip of the optical fiber was 30 uW (470 nm) and 15 uW (410 nm). ΔF/F was calculated according to (470 nm signal-fitted 410 nm signal)/(median of the photometry signal).

2.4. Histologic analysis

To perform Hematoxylin and eosin (H&E) staining of liver, adipose tissues and pancreas, these tissues were dissected, fixed in 4 % paraformaldehyde (PFA, P0099, Beyotime Biotechnology) for at least 24 h in room temperature, and embedded in paraffin. Then paraffin tissue sections were stained with H&E or analyzed by immunohistochemistry (IHC).

For immunofluorescence analysis, under unanesthetized condition, mice were perfused with 30 ml 0.9 % NaCL, and then fixed with 50 ml 4 % PFA through transcardial perfusion. Whole brains were collected, post-fixed with 4 % PFA for 12h, dehydrated using graded sucrose solutions (20%-24h, 30%-24h) and sectioned at a 30 mm thickness on a cryostat (CM1950, Leica, Wetzlar, Germany). Tissue sections were blocked for 30 min at room temperature with 5 % donkey or sheep serum in PBS with 0.3 % Triton X-100, and then incubated with rabbit

anti-GPSM1 (11483-1-AP, Proteintech, 1:100), rabbit anti-p-STAT3 (9131, CST, 1:400) (For p-STAT3 staining, brain slices were firstly treated with 0.5 % NaOH and 0.5 % H2O2 in PBS for 20 min, followed by 0.3 % glycine for 10 min, and then 0.03 % SDS for 10 min), rabbit anti-c-FOS (2250, CST, 1:1000), rabbit anti-P62 (18420-1-AP, Proteintech, 1:500) or sheep anti-α-MSH (AB5087, Sigma-Aldrich, 1:1000) primary antibodies at 4 °C overnight, and then incubated corresponding fluorophore-conjugated secondary antibodies from Thermo Fisher Scientific at room temperature for 1 h. DAPI was used for counterstaining cell nuclei at room temperature for 5 min. Images were acquired with an LSM980 confocal microscope (Carl Zeiss, Jena, Germany) and processed using Adobe photoshop CC 2019. The number of GPSM1, p-STAT3, c-FOS, mCherry, and double-positive cells were manually counted on one side of Arc nucleus in a representative image acquired from each mouse. The fluorescence intensity of α-MSH was determined with ImageJ software (Ver. 1.52, National Institutes of Health).

2.5. RNA extraction and RT PCR

RNA of mouse tissue was extracted using the RNeasy Plus Universal Kit (1023537, QIAGEN), and then reverse-transcribed into cDNA using the PrimeScript RT reagent kit (RR047A, Takara). SYBR Green Master Mix (01000432, Applied Biosystems) was used for RT- PCR analyses through a QuantStudio Real-Time PCR System (Applied Biosystems). Primers are listed in Supplementary Table 1 (Table S1).

2.6. Protein extraction and western blot analysis

Protein of tissues and cells were extracted using a RIPA buffer (Beyotime Biotechnology) containing protease and phosphatase inhibitors (Roche), and quantified by the BCA protein assay kit (Beyotime). Cleared supernatants were electrophoresed in 8%—15 % SDS—PAGE gels, and wet-transferred to nitrocellulose filter membrane (Millipore). Then, blocking the blots for 1 h at room temperature by using 5 % skim milk or bovine serum albumin (CST), followed by incubation with rabbit anti-UCP1 (ab10983, Abcam, 1:1000), mouse anti-TH (MAB318, Sigma-Aldrich, 1:1000), mouse anti-Tubulin (T9026, Sigma-Aldrich, 1:1000), rabbit anti-GPSM1 (11483-1-AP, Proteintech, 1:1000), mouse anti-P62 (ab56416, Abcam, 1:1000), rabbit anti-LC3B (3868, CST, 1:1000), rabbit anti-PI3K (4757, CST, 1:1000), rabbit anti-AKT (9272, CST, 1:1000), rabbit anti-pAKT (9271, CST, 1:1000), rabbit anti-mTOR (2972, CST, 1:1000), rabbit anti-pmTOR (2971, CST, 1:1000), rabbit anti-STAT3 (9139, CST, 1:1000), rabbit anti-pSTAT3 (9131, CST, 1:1000), rabbit anti-β-actin (4970, CST, 1:1000), and mouse anti-GAPDH (sc-32233, Santa Cruz Biotechnology, 1:1000) antibodies overnight at 4 °C. In the next day, incubated the blots with horseradish peroxidase—conjugated secondary antibody (anti—rabbit IgG, HRP-linked antibody, 7074, or anti—mouse IgG, HRP-linked antibody, 7076, CST) for 1 h at room temperature. To capturing the protein bands, ChemiDoc Imaging System (BioRad) was used through ECL Chemiluminescent Kit (Millipore). Image Lab software version 6.0 for acquisition of images from Western blot. Band intensities were quantified using ImageJ (National Institutes of Health) version 1.52.

2.7. Cell culture and treatments

mHypoE-N43/5 cells were maintained in Dulbecco's modified Eagle's medium (DMEM, 11995, GIBCO) supplemented with 10 % fetal bovine serum and 1 % penicillin/streptomycin (P/S, 15140-122, GIBCO) at 37 °C with 5 % CO2. For *GPSM1* knockdown, mHypoE-N43/5 cells (1×10^6 to 2×10^6 cells) were prepared and infected for 72 h at a multiplicity of infection (MOI) of 30 with lentivirus-sh*GPSM1* (Shanghai GeneChem). For overexpression experiments, mHypoE-N43/5 cells were transfected with Flag or *GPSM1*-Flag expression plasmid (The full-length mouse *GPSM1* gene containing a Flag-tag at C-terminus was cloned into pcDNA3.1) using Lipofectamine 3000 (L3000015, Invitrogen) according to the manufacturer's instructions. To exploring autophagy changes, HBSS (14025092, GIBICO) was used to induce starvation for 4 h, BafA1 (100 nM, 4 h, 196000, Sigma-Aldrich) was used to inhibit autophagosome-lysosome fusion. Rapamycin (1uM, 3 h, V900930, Sigma-Aldrich) was used to activate autophagy. Leptin (100 uM, 30 min, 498-OB-05M, R&D) was used to activate leptin signaling.

2.8. Statistical analysis

All data in this study are presented as means with standard errors (SEs). Differences between groups were analyzed either by the unpaired two-tailed Student's t test, or two-way ANOVA comparison test with Sidak's multiple-comparisons test, Oxygen consumption (ml/h) and energy expenditure (kcal/24h) values were correlated to the body weight by using analysis of co-variance (ANCOVA), in GraphPad Prism (version 9.1.0; GraphPad Software Inc.). $P < 0.05$ was considered statistically significant.

3. RESULTS

3.1. Deletion of GPSM1 in POMC neurons protects against obesity

To explore whether GPSM1 in POMC neurons regulates obesity, we intercrossed mice bearing a conditional loxP-flanked allele of *GPSM1* (*GPSM1*$^{f/f}$, LoxP, used as control mice) with the *POMC*-Cre line to create POMC-neuron-specific *GPSM1*-knockout (*GPSM1*^{PKO}, PGKO) mice. For determination of the specificity and efficiency of *GPSM1* deletion, PGKO mice were intercrossed with Rosa26-tdTOMATO (Ai9) mice to generate PGKO/Ai9 mice, for labeling of the POMC neurons *in vivo*. Immunofluorescence (IF) staining showed that GPSM1 was colocalized with POMC-expressing neurons in ARC of control mice, but this colocalization was largely reduced in PGKO/Ai9 mice, as evaluated by counting the number of GPSM1-positive POMC neurons (Figure 1A). Because Cre recombinase expression in the pituitary is also driven by POMC promoter, we examined serum corticosterone contents secreted from pituitary to examine whether the function of the pituitary-adrenal axis was affected. Our results showed that serum corticosterone and the morphology of adrenal gland were compatible between the two groups (Figure S1A, B). Moreover, the population size and distribution of POMC neurons throughout ARC of PGKO and control mice had no difference (Figure S1C, D), which indicated that GPSM1 did not influence POMC neuron differentiation and survival.

In the setting of Normal Chow Diet (NCD) feeding for 20 weeks, no significant differences were detected in murine body weight and adiposity between the two groups (Figure S2A—G). At 11 weeks of High-fat Diet (HFD) challenge, the mice lacking *GPSM1* exclusively in POMC neurons were partially resistant to obesity, exhibiting much lower body weights than control mice (Figure 1B), which was accompanied with decreased total fat mass but unchanged lean mass confirmed by Dual Energy X-ray Absorptiometry (Figure 1C). Moreover, the fat-pad weights, including inguinal WAT (iWAT), epididymal WAT (eWAT) and brown adipose tissue (BAT) were all decreased in PGKO mice, compared with that in LoxP mice (Figure 1D). Notably, hematoxylin and eosin (H&E) staining showed that PGKO mice had smaller adipocyte size of iWAT, eWAT and BAT (Figure 1E—G). Altogether, these results suggest that ablation of *GPSM1* in POMC neurons reduces fat storage and protects against obesity.

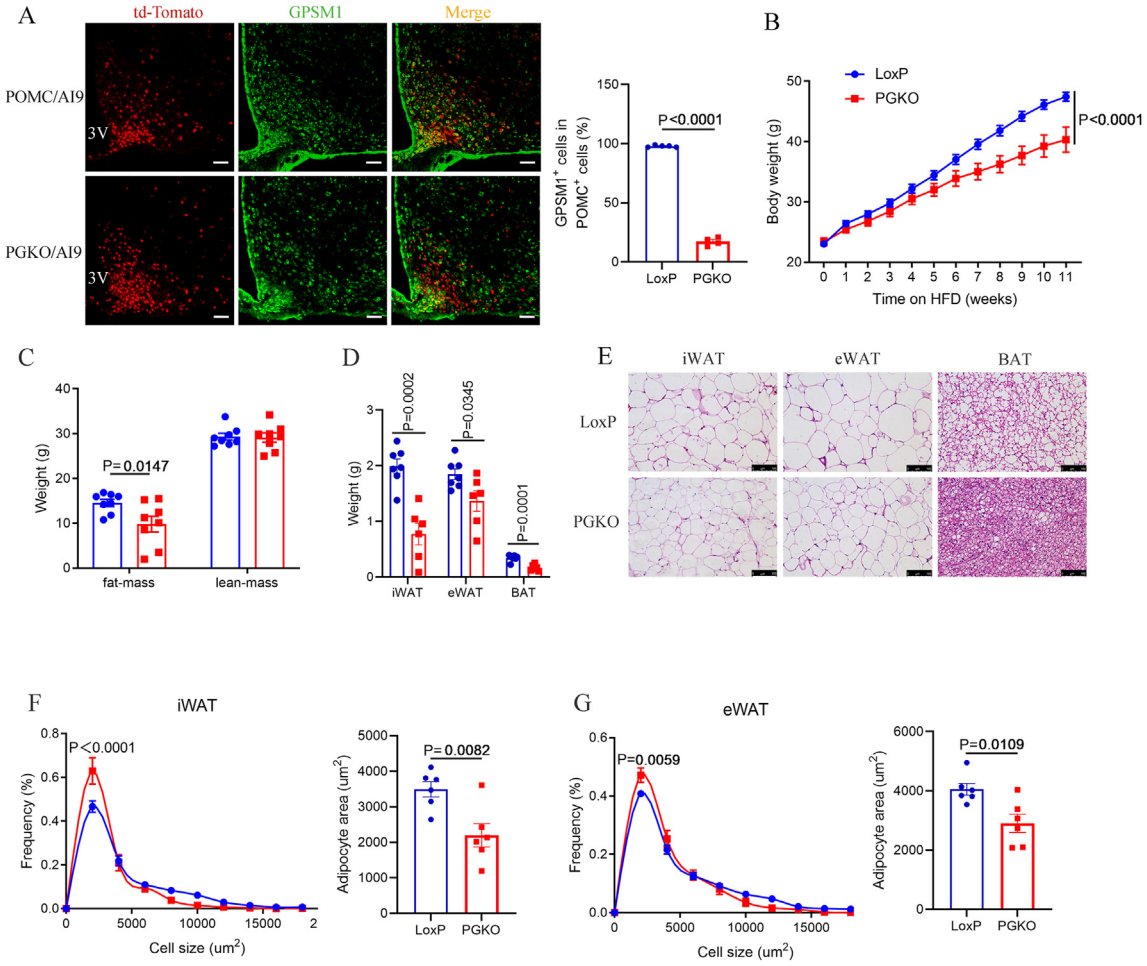

Figure 1: Deletion of GPSM1 in POMC neurons protects male mice from diet-induced obesity. (A) Representative immunofluorescence (IF) images and statistical analysis of the percentage of GPSM1 (green) in POMC neurons (red) in the arcuate nucleus (ARC) of POMC/Ai9 (n = 4) and PGKO/Ai9 (n = 4) mice (CD 8w). 3V, third ventricle. Scale bar, 100 μm. (B) Body weight curve of LoxP (n = 9) and PGKO (n = 8) mice (HFD 11w). (C) Weights of body fat mass and lean mass of LoxP (n = 8) and PGKO (n = 8) mice (HFD 14w). (D) Weights of inguinal white adipose tissue (iWAT), epididymal white adipose tissue (eWAT) and brown adipose tissue (BAT) of LoxP (n = 7) and PGKO (n = 6) mice (HFD 14w). (E) Representative H&E-stained sections of iWAT, eWAT and BAT (HFD 14w). Scale bar, 100 μm. (F–G) Frequency distribution and area of adipocytes in iWAT and eWAT from LoxP (n = 6) and PGKO (n = 6) mice. Scale bar, 100 μm. Data are shown as mean ± SEM. Statistical analyses were performed by two-way analysis of variance (ANOVA) with Sidak's multiple-comparisons test (B, F, and G) or unpaired two-tailed Student's t-test (A, C and D).

3.2. Deletion of GPSM1 in POMC neurons improves glucose intolerance and lipid dysregulation

HFD-induced obesity is normally accompanied by glucose intolerance and lipid dysregulation [26,27], we therefore investigated the impact of POMC GPSM1 on systemic glucose and lipid metabolism. As expected, PGKO mice showed improved glucose tolerance and insulin sensitivity as demonstrated by glucose tolerance tests (GTTs) and insulin tolerance tests (ITTs), respectively (Figure 2A,B). Moreover, the levels of fasting blood glucose and serum insulin were lower in PGKO compared with control mice maintained on an HFD (Figure 2C,D). Consistently, the size of pancreatic islet of PGKO group was also smaller (Figure 2E). In addition, we observed that PGKO mice were significantly protected from HFD-induced hepatic steatosis, with lower liver weights and hepatic lipid accumulation showed by H&E and Oil Red O staining (Figure 2F–H). Consistently, PGKO mice indeed had lower serum AST, ALT, LDL and cholesterol levels (Figure 2I-L). However, Upon HFD for 4 weeks, at the time when LoxP and PGKO mice had comparable body weights, no differences were observed in the GTTs and ITTs between the two groups (Figure S3A–E), indicating that the improved glucose and insulin tolerance in PGKO mice might be due to their lower body weights. Overall, the results demonstrate that GPSM1 in POMC neurons plays an important role in systemic glucose and lipid metabolism.

3.3. Deletion of GPSM1 in POMC neurons improves energy expenditure by promoting thermogenesis in BAT

We next sought to elucidate the mechanisms underlying the improved metabolic phenotypes of PGKO mice. We found that PGKO mice had a reduced daily food intake and higher O_2 consumption, CO_2 production and energy expenditure under an HFD, compared with the control group (Figure 3A–C, Figure S4A–D). No difference in total physical activity was observed between LoxP and PGKO mice (Figure S4E). Moreover, rectal temperature was notably higher in PGKO than that of controls (Figure 3D), which implicates improved thermogenesis in

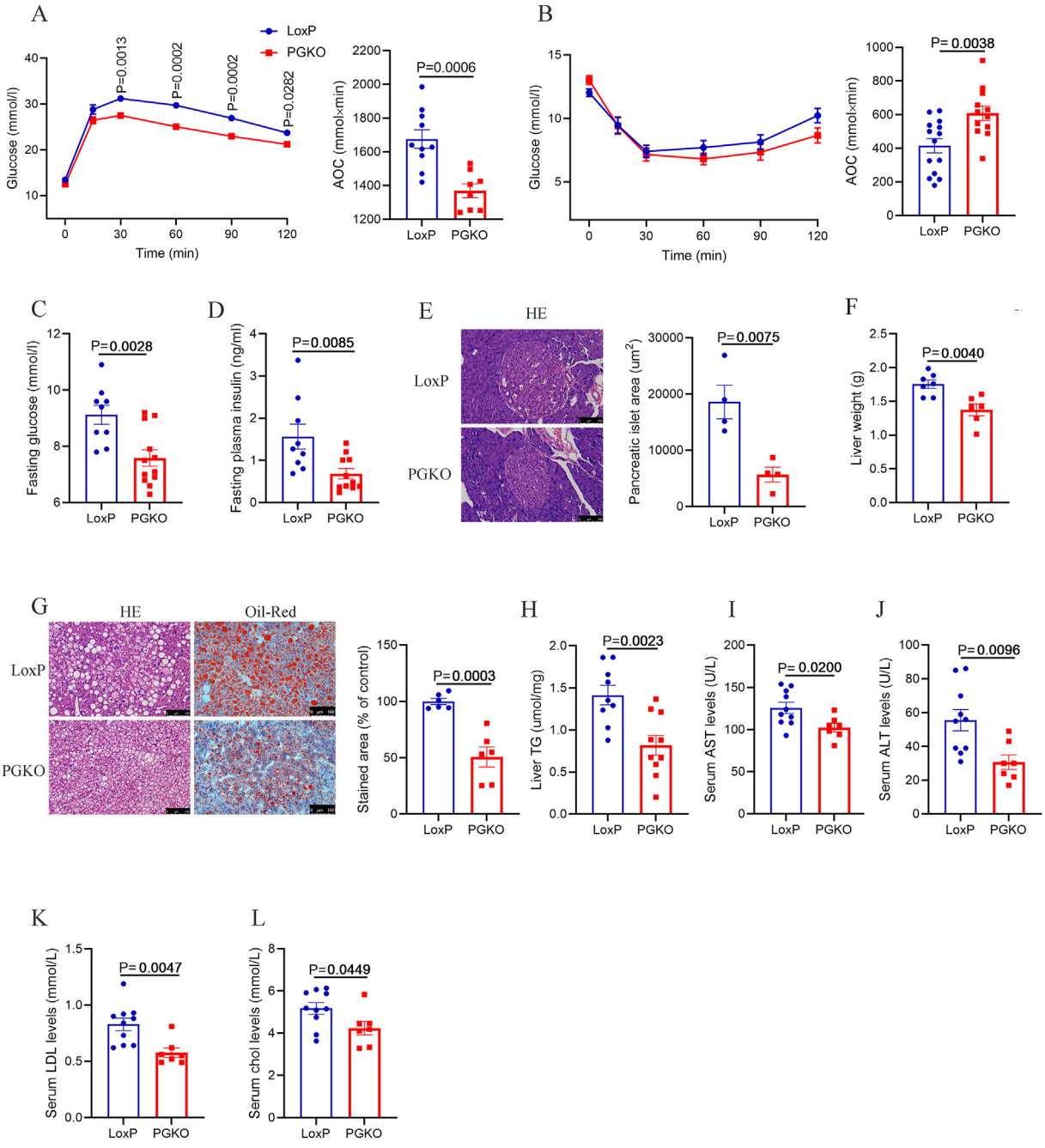

Figure 2: Deletion of GPSM1 in POMC neurons improves glucose tolerance, insulin sensitivity and liver steatosis in male mice on an HFD. (A) Glucose tolerance tests in LoxP (n = 16) and PGKO mice (n = 13) (HFD 10w). AOC, area under the curve. (B) Insulin tolerance tests in LoxP (n = 14) and PGKO (n = 12) mice (HFD 10w). AOC, area under the curve. (C) Fasting glucose levels in LoxP (n = 9) and PGKO (n = 12) mice (HFD 14w). (D) Fasting insulin levels in LoxP (n = 9) and PGKO (n = 11) mice (HFD 14w). (E) Representative H&E-stained sections of the pancreas and the mean area of pancreatic islet of LoxP (n = 4) and PGKO (n = 4) mice (HFD 14w). (F) Liver weights of LoxP (n = 7) and PGKO (n = 6) mice (HFD 14w). (G) Representative images of H&E staining (left) and Oil Red O (right) staining of liver sections and quantification of Oil Red O staining in LoxP (n = 6) and PGKO (n = 6) mice (HFD 14w). (H) Quantification of hepatic triglycerides in LoxP (n = 9) and PGKO (n = 10) mice (HFD 14w). (I–L) Serum levels of ALT, AST, Low Density Lipoprotein (LDL), and cholesterol (CHOL) in LoxP (n = 10) and PGKO (n = 7) mice (HFD 14w). Scale bars, 100 μm. Data are shown as means ± SEM. Statistical analyses were performed by two-way analysis of variance (ANOVA) with Sidak's multiple-comparisons test (A and B) or unpaired two-tailed Student's t-test (C–L).

PGKO mice. Consistently, the thermogenic markers, including mRNA levels of *Ucp-1*, *Pgc-1α*, *Dio2*, *Cox5a*, *Cox7a* and *Cox8b*, as well as the protein levels of UCP-1, revealed by immunohistochemistry (IHC) and western blot (Figure 3E–G), were significantly up-regulated in the BAT of PGKO mice.

As activation of sympathetic nervous system (SNS) could increase BAT thermogenesis [28,29], we next assessed whether ablation of *GPSM1* in POMC neurons impacted the delivery of the SNS signals in the brain to BAT. As the IHC and western blot showed, the marker of activated SNS, tyrosine hydroxylase (TH), an enzyme required for the synthesis of catecholamines, was significantly higher in BAT of PGKO mice (Figure 3F,G), companied by elevated serum noradrenaline (NE) levels (Figure 3H). These data suggests that *GPSM1* ablation in POMC neurons improves sympathetic nerve activity related to BAT.

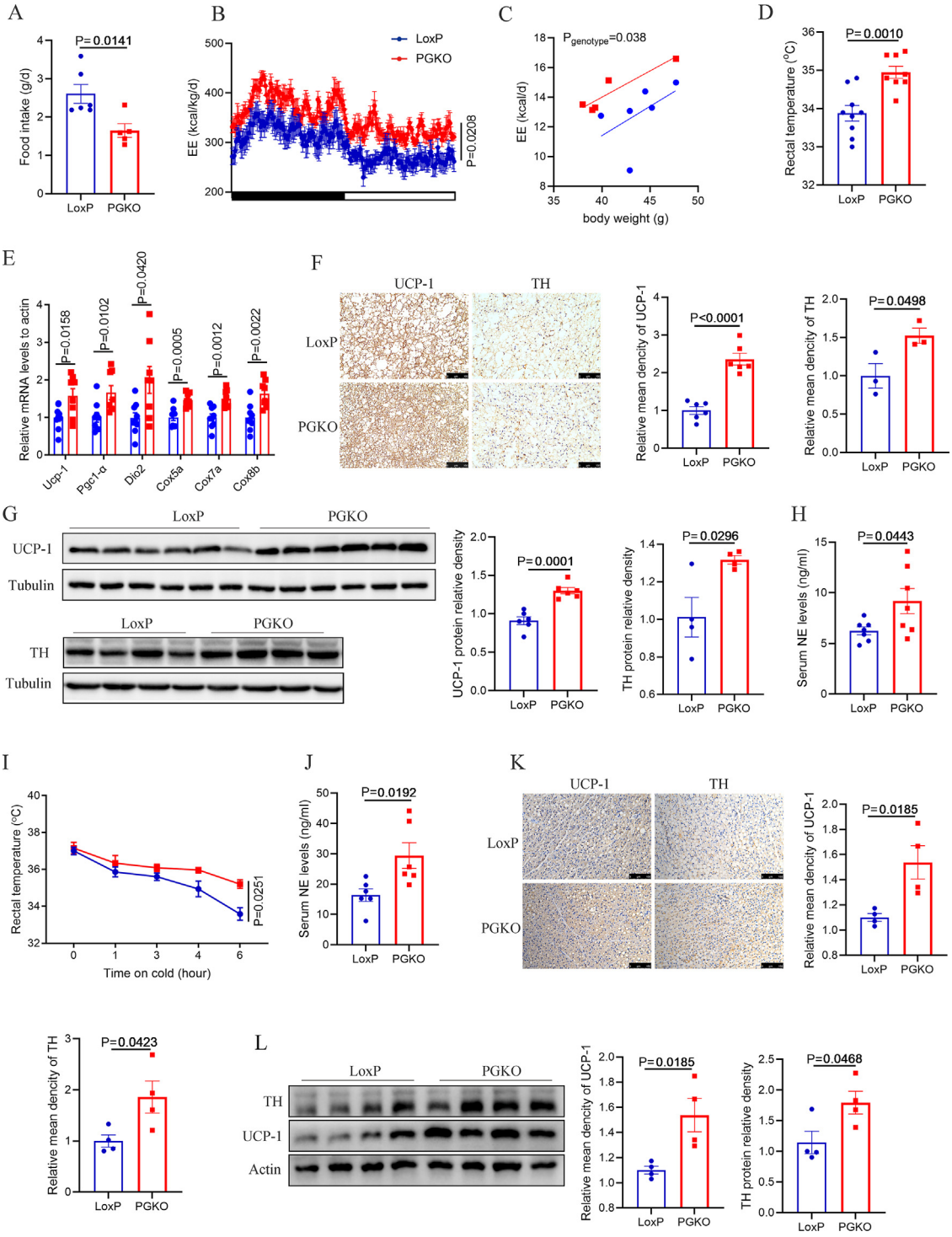

Figure 3: Deletion of GPSM1 in POMC neurons increases energy expenditure by enhancing sympathetic nervous system-dependent thermogenesis in BAT of male mice on an HFD. (A) Daily food intake of LoxP (n = 6) and PGKO (n = 5) mice (HFD 13w). (B–C) Energy expenditure (kcal/kg/d) and ANCOVA analysis of the energy expenditure (kcal/d) versus body weight of LoxP (n = 6) and PGKO (n = 5) mice (HFD 11w). (D) Rectal temperature of LoxP (n = 9) and PGKO (n = 8) mice at room temperature (RT) (HFD 13w, 2 p.m.). (E) Relative mRNA expressions of thermogenic genes in BAT from LoxP (n = 9) and PGKO (n = 7) mice at RT (HFD 14w). (F) Representative IHC images and quantification of UCP-1 (left, n = 6) and TH (right, n = 3) in BAT (HFD 14w). (G) Western blot analysis and quantification of UCP-1 (n = 6) and TH (n = 4) levels in BAT at RT (HFD 14w). (H) ELISA analysis of noradrenaline (NE) content in serum from LoxP (n = 7) and PGKO (n = 7) mice at RT (HFD 14w). (I) Rectal temperature upon cold exposure (CE) of LoxP (n = 5) and PGKO (n = 6) mice (CD 12w). (J) ELISA analysis of NE content in serum from LoxP (n = 6) and PGKO (n = 6) mice upon CE (CD 12w). Scale bar, 100 μm. (K) Representative IHC images and quantification of UCP-1 (left, n = 4) and TH (right, n = 4) in BAT upon CE (CD 12w). (L) Western blot analysis and quantification of UCP-1 (n = 4) and TH (n = 4) levels in BAT upon CE (CD 12w). Protein levels were normalized to a loading control of each sample. Data are shown as mean ± SEM. Statistical analyses were performed by two-way analysis of variance (ANOVA) with Sidak's multiple-comparisons test (B, C and I) or unpaired two-tailed Student's t-test (A, D, E-H, and J-L).

Cold can induce BAT thermogenesis by promoting SNS activity [30,31]. We next explored whether PGKO mice exhibited improved thermogenesis under cold exposure. After 6 h of cold exposure (4 °C), PGKO mice had a higher core temperature and serum NE levels than did control mice (Figure 3I,J). The expression of UCP1 and TH were also induced after *GPSM1* deletion in POMC neurons (Figure 3K,L). Together, these findings elucidate that GPSM1 in POMC neurons impairs thermogenesis in BAT via defective SNS activity, thereby impairing whole-body energy expenditure.

Furthermore, as POMC neurons are sexually dimorphic, we next explored whether the effects of GPSM1 in POMC neurons persisted in female mice. Upon an HFD for 6 weeks, the PGKO female mice exhibited a lower body weight, as well as improved glucose tolerance and insulin sensitivity, compared with their counterparts (Figure 4A–D). In addition, the PGKO female mice also had elevated O_2 consumption, CO_2 production and energy expenditure, which were in agreement with the phenotype of male mice (Figure 4E–H).

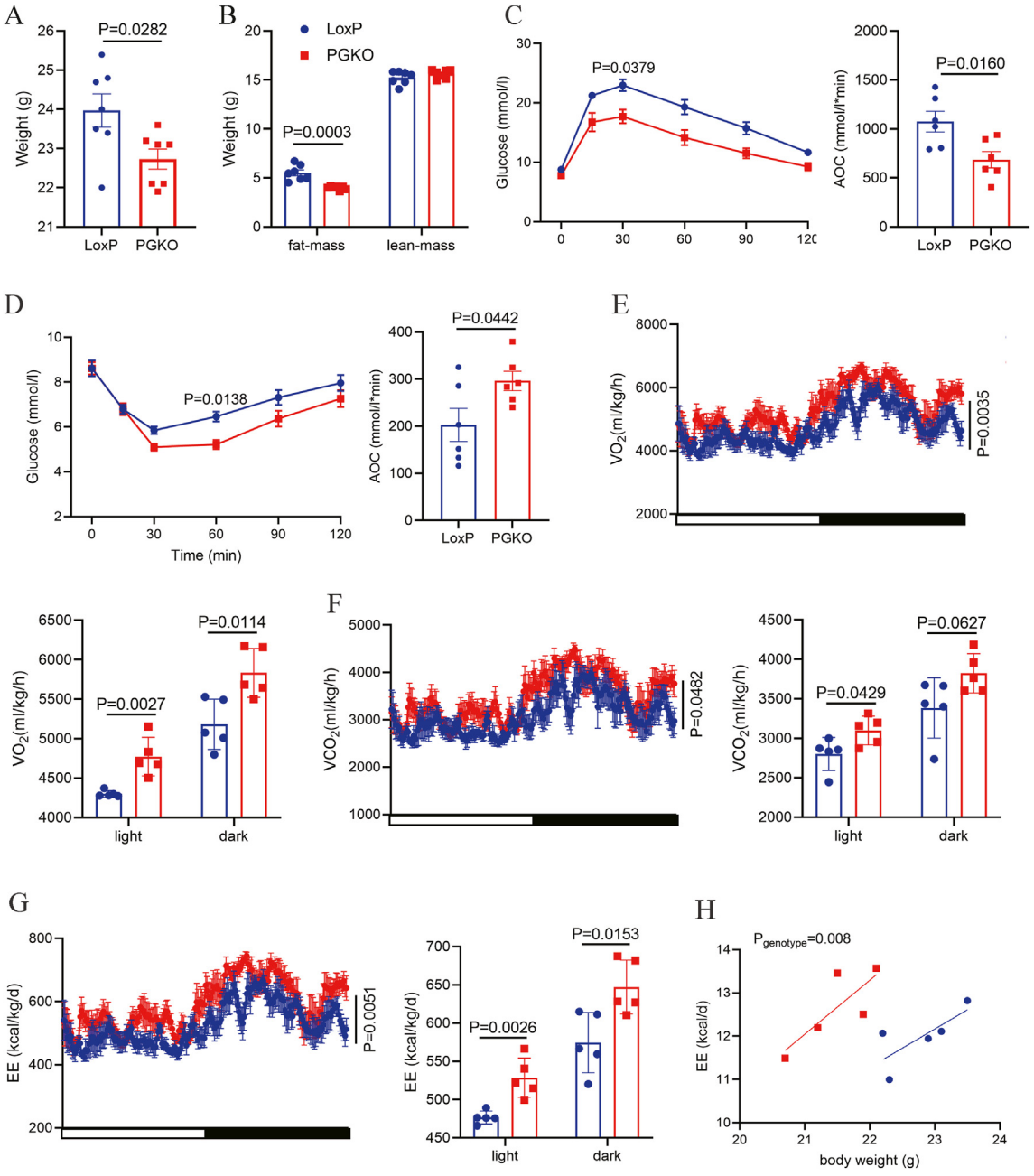

Figure 4: Deletion of GPSM1 in POMC neurons protects female mice from diet-induced obesity. (A) Body weights of LoxP (n = 7) and PGKO (n = 7) female mice (HFD 6w). (B) Weights of body fat mass and lean mass of LoxP (n = 7) and PGKO (n = 7) mice (HFD 6w). (C) Glucose tolerance tests in LoxP (n = 6) and PGKO female mice (n = 6) (HFD 6w). AOC, area under the curve. (D) Insulin tolerance tests in LoxP (n = 6) and PGKO (n = 6) female mice (HFD 6w). AOC, area under the curve. (E–H) O_2 consumption, CO_2 production and energy expenditure of LoxP (n = 5) and PGKO (n = 5) mice (HFD 6w). Statistical analyses were performed by two-way analysis of variance (ANOVA) with Sidak's multiple-comparisons test (C–G) or unpaired two-tailed Student's t-test (A–G).

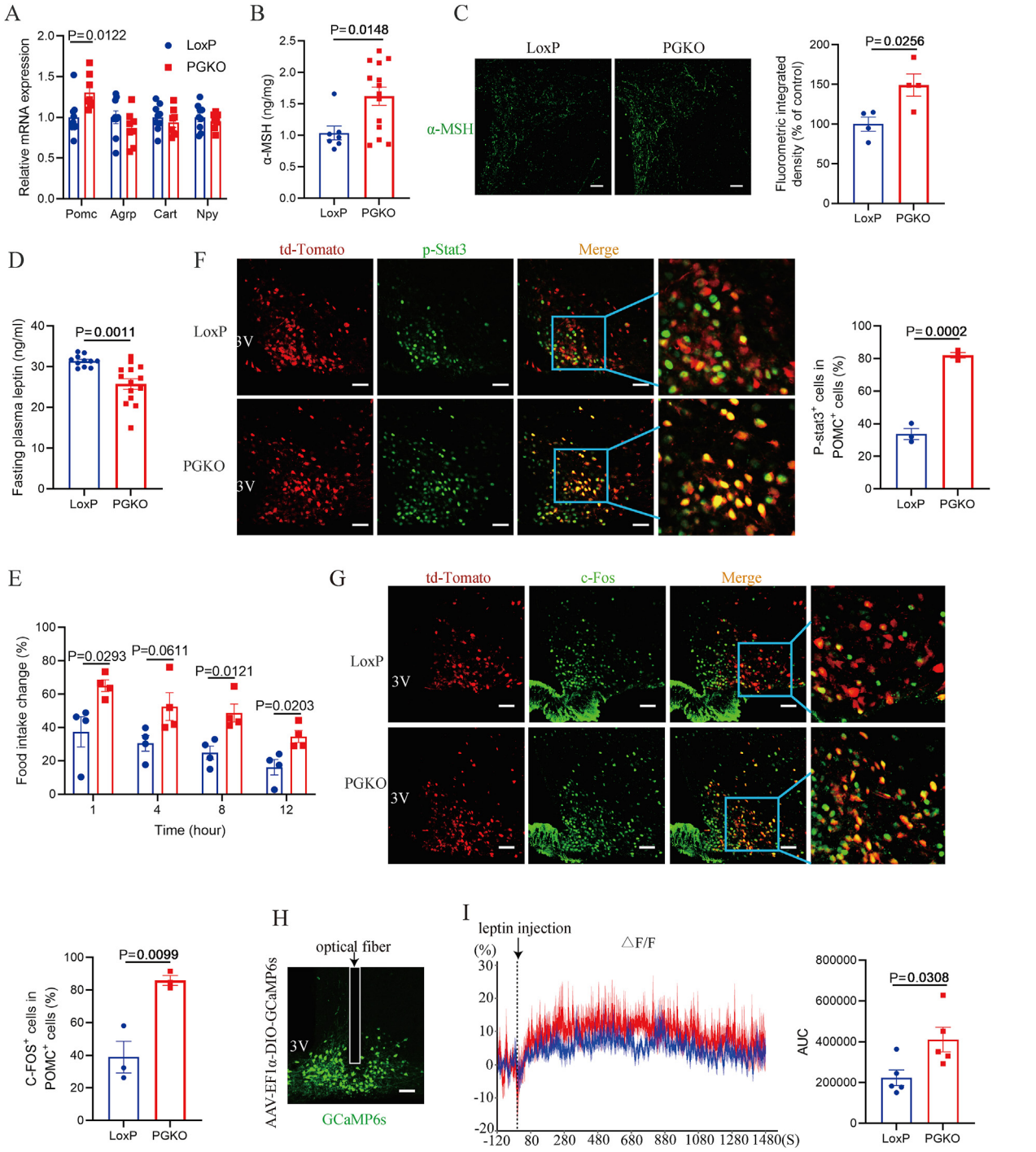

Figure 5: Deletion of GPSM1 in POMC neurons increases POMC expression and α-MSH production and improves HFD-induced leptin resistance. (A) Relative mRNA expressions of neuropeptide in LoxP (n = 9) and PGKO (n = 8) mice (HFD 14w, fed state). (B) ELISA analysis of α-MSH contents in hypothalami from LoxP (n = 7) and PGKO (n = 14) mice (HFD 14w, fed state). (C) Representative images and quantification of IF images of α-MSH in paraventricular nucleus (PVN) of LoxP (n = 4) and PGKO (n = 4) mice (HFD 14w, fed state). (D) Fasting plasma leptin levels in LoxP (n = 14) and PGKO (n = 14) mice (HFD 11w). (E) Food intake change after i.p. injected with leptin in LoxP (n = 4) and PGKO (n = 4) mice (HFD 10w). (F—G) Representative images and quantification of IF staining of p-STAT3 (green) and c-FOS (green) in POMC neurons (red) of LoxP (n = 3) and PGKO (n = 3) mice after i.p. injected with leptin for 45 min (HFD 12w). 3V: third ventricle; Scale bar, 50 μm; (H—I) Calcium signal traces and AUC from POMC neurons in POMC-Cre (n = 5) and PGKO mice (n = 5) (HFD 8w). Data are shown as mean ± SEM. Statistical analyses were performed by unpaired two-tailed Student's t-test (A-G and I).

3.4. Deletion of GPSM1 in POMC neurons increases α-MSH production and improves leptin sensitivity

To investigate the mechanisms underlying increased SNS activity in PGKO mice, we first assessed neuro-peptides expression in the hypothalamus. Under an HFD, the mRNA levels of AGRP and NPY were comparable between LoxP and PGKO mice, but the expression levels of POMC was upregulated in the hypothalamus of PGKO mice (Figure 5A). Additionally, when GPSM1 was knocked down by infecting with

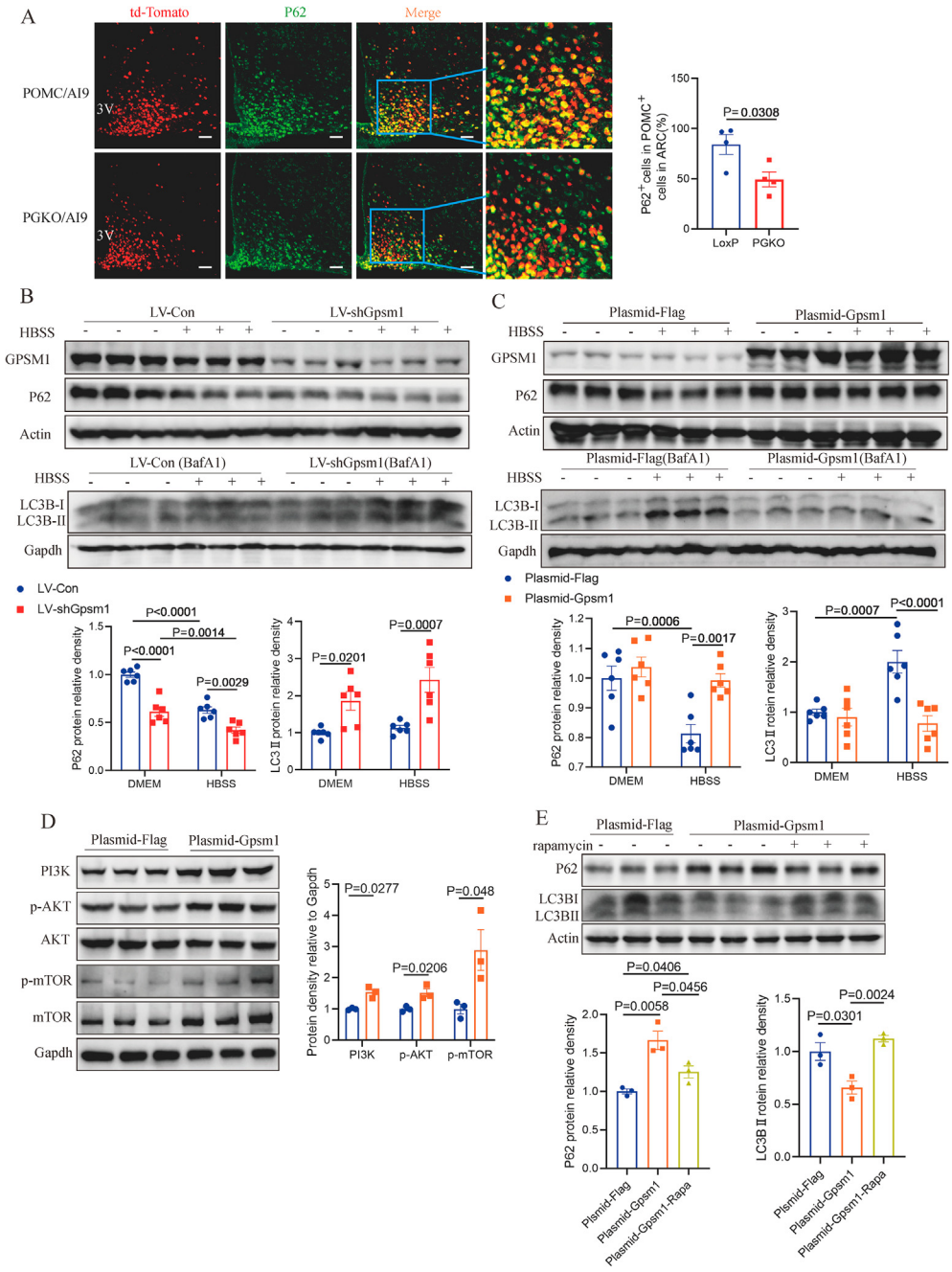

Figure 6: Deletion of GPSM1 in POMC neurons increases autophagy in POMC neurons. (A) Representative IF images and quantification of P62 (green) in POMC neurons (red) in the arcuate nucleus (ARC) of POMC/Ai9 (n = 3) and PGKO/Ai9 (n = 3) mice (HFD 12w), merge (yellow). 3V, third ventricle. Scale bar, 100 μm. (B) Western blot analysis and quantification of P62 and LC3B levels in mHypoE-N43/5 cell lines with *GPSM1* knockdown. (C) Western blot analysis and quantification of P62 and LC3B levels in mHypoE-N43/5 cell lines with *GPSM1* overexpression. (D) Western blot analysis of PI3K, p-AKT (ser473), AKT, p-mTOR (ser2448) and mTOR and quantification of PI3K, p-AKT (ser473), and p-mTOR (ser2448) levels in mHypoE-N43/5 cell lines with *GPSM1* overexpression. (E) Western blot analysis and quantification of P62 and LC3B levels in mHypoE-N43/5 cell lines after treatment of rapamycin with *GPSM1* overexpression. Protein levels were normalized to a loading control of each sample. Data are shown as mean ± SEM. Statistical analyses were performed by unpaired two-tailed Student's t-test (A–E).

lentivirus-shGPSM1, in an established POMC cell line-mHypoE-N43/5 cells, the same trend of POMC gene expression was observed (Figure S5A). α-MSH is the production of the precursor POMC peptide and post-translational cleavage of POMC to generate α-MSH needs several convertases, however, we found no differences in these convertases between LoxP and PGKO mice (Figure S5B). Next, we detected α-MSH concentrations in the hypothalamus and found PGKO mice had a higher level of α-MSH than that of controls (Figure 5B). As α-MSH produced from POMC neurons transports to paraventricular nucleus (PVN) of hypothalamus to function, we used IF staining

showing that PGKO mice had increased α-MSH staining in the PVN (Figure 5C). In short, these results showed PGKO mice had increased POMC expression and α-MSH production.

Leptin receptor, which is abundantly expressed in hypothalamus, especially in POMC-expressing neurons, plays a vital role in energy expenditure and food intake [32]. Obesity is often accompanied by leptin resistance and gives rise to a disturbed effects on metabolism [33]. As expected, plasma fasting leptin levels were lower in PGKO mice after a 11-weeks HFD (Figure 5D). Additionally, to further examine the effect of POMC GPSM1 on leptin sensitivity, we i.p. administered saline and leptin to PGKO and control mice, and then compared the effects of leptin on reducing food intake at a series of time points. We found that PGKO mice had a more food intake reduction after leptin injection than their littermates (Figure 5E). Consistently, leptin injection induced more signals of phosphorylated STAT3 (p-STAT3) in POMC neurons of PGKO mice, the maker of leptin signaling activation (Figure 5F). Further, to explore the improved leptin sensitivity observed after POMC *GPSM1* deficiency was of primary cause or secondary to the improved metabolic phenotypes, we performed the leptin sensitivity test in mice under an HFD for 4 weeks, at the time when the body weight and food intake of LoxP and PGKO mice were comparable. The results revealed that the enhanced anorectic effects of exogenous leptin were still more significant in PGKO mice (Figure S5C, D).

Finally, in respect to whether the activity of POMC neurons was altered after GPSM1 loss, we first used IF staining of c-FOS and the results revealed that the c-FOS signals were obviously higher in *GPSM1*-ablation POMC neurons (Figure 5G), indicating *GPSM1* loss could increase the activity of POMC neurons excited by leptin. Moreover, to further demonstrate that POMC neuron activity was increased in the PGKO mice *in vivo*, we employed a Cre-dependent expression of the calcium sensor GCaMP6s in POMC neurons to record *in vivo* calcium transients. The response of POMC neurons to leptin was significantly increased after knocking out *GPSM1* from POMC neurons (Figure 5H,I), supporting the notion that depletion of *GPSM1* in POMC neurons indeed increased the activity of POMC neurons excited by leptin. Collectively, the results indicate that the depletion of *GPSM1* in POMC neurons could improve leptin sensitivity.

3.5. Deletion of GPSM1 in POMC neurons elevates autophagy *in vivo* and *in vitro*

As GPSM1 has been reported to play a role in the progression of autophagy [34] and autophagy is a crucial regulator in POMC neuron activity [35], therefore, we hypothesized that the improved metabolic phenotypes of PGKO mice might attribute to the changed autophagy in POMC neurons. To test this possibility, we detected the p62 protein, a negative autophagy marker, in POMC neurons by IF staining. As expected, p62 staining in POMC neurons were weakened upon deletion of *GPSM1* in POMC neurons after HFD for 12 weeks (Figure 6A). Notably, the same trend of P62 also existed in mice under HFD for 4 weeks (Figure S5E), at the time when the body weight and glucolipid metabolism had no difference between two groups. It suggested that the increased autophagy preceded the induction of improved metabolic phenotypes. Correspondingly, *in vitro* studies, the increased LC3B-II and decreased p62 protein levels were observed when GPSM1 protein levels were knocked down by infecting with lentivirus-shGPSM1, compared with control lentivirus, in mHypoE-N43/5 cells (Figure 6B, Figure S5F). Additionally, the opposite effects were detected when GPSM1 was overexpressed (Figure 6C, Figure S5G).

As PGKO mice exhibited improved leptin sensitivity and autophagy, and the references have reported that leptin and autophagy signaling interacted with each other [36—38], we further treated POMC cells with leptin and found that GPSM1 could also regulate leptin signaling in a cell-autonomous manner (Figure S5H). In respect to POMC neurons, the inhibited autophagy, such as loss of autophagy-related 5, 7, 12 proteins (ATG5, ATG7, ATG12) in POMC neurons, might be the initial cause of impaired leptin signaling [35,39,40]. Therefore, we further explored whether the decreased leptin sensitivity came from the inhibited autophagy in *GPSM1* overexpression cells. Results showed that autophagy activation stimulated by rapamycin could abolish the inhibitory effect of *GPSM1* overexpression on leptin signaling (Figure S5H), indicating that the leptin signaling regulated by GPSM1 in POMC neurons was, at least, partly due to the regulation of GPSM1 on autophagy pathway.

Next, we aimed to determine the specific mechanisms involved in the regulation of GPSM1 on autophagy. As the kinase mammalian target of rapamycin (mTOR)-a downstream target of the phosphatidylinositol 3 kinase (PI3K) and kinase AKT (AKT) pathway, is an important factor to regulate autophagy [41], and study reported that GPSM1 had an effect on PI3K/AKT/mTOR signaling in a colorectal cancer model [42], therefore, we supposed that the regulation of GPSM1 on autophagy in POMC neurons might depend on the PI3K/AKT/mTOR signaling. As expected, the protein abundance of PI3K, p-AKT and p-mTOR were significantly increased when overexpressing GPSM1 in the mHypoE-N43/5 cells (Figure 6D). Conversely, administrating the inhibitor of mTOR, rapamycin, could restore autophagy in the GPSM1-overexpression group (Figure 6E). The results indicate that the PI3K/AKT/mTOR axis as a molecular component preferentially regulate GPSM1-induced autophagy inhibition in the POMC neurons.

4. DISCUSSION

In this study, we elucidate a novel function of GPSM1 expressed in POMC neurons in the regulation of whole-body energy balance. We found that deletion of *GPSM1* in POMC neurons helped to prevent HFD-induced obesity, glucose dysregulation, insulin resistance and associated metabolic disorders, which was due to stimulated BAT thermogenesis via increasing its sympathetic innervation and activity. Mechanistically, we demonstrated that GPSM1 affected the activation of POMC neurons through regulation of autophagy and leptin signaling in the hypothalamus.

GPSM1 is abundantly expressed in the brain [21]. Previous studies have proved the potential role of GPSM1 in neural precursor cell division and differentiation, as well as drug and cocaine-seeking behavior [23,24]. However, whether GPSM1 has impact on hypothalamic nuclei, especially the ARC, still remains unknown. Moreover, studies have suggested that animals exposed to various addictive drugs may alter hypothalamic POMC transcripts levels, similar to an HFD feeding [9,43,44]. Therefore, we investigated the role of GPSM1 in the POMC neurons in the development of obesity. As expected, herein, deletion of *GPSM1* in POMC neurons results in a lean phenotype in mice maintained on an HFD. As the hypothalamus contains multiple types of neural populations, and the roles of these cells in modulating energy homeostasis are diverse and complex, further studies are warranted to focus on the crucial effects of GPSM1 in other neural populations.

HFD-induced obesity is normally accompanied by glucose intolerance and insulin resistance [26,27]. Our study found deficiency of *GPSM1* in POMC neurons improved glucose intolerance and insulin resistance on an HFD, which could be a consequence of the reduced fat mass in PGKO mice, as no differences in glucolipid metabolism indexes were observed between PGKO and control mice under a CD or an HFD for 4

weeks when there was no difference in body weight. An aged mouse model will be helpful to identify the influence of intrinsic metabolic state on the function of GPSM1 in POMC neurons, as aging itself causes many physiological changes in body composition, resulting in metabolic diseases.

Because energy homeostasis is maintained by a balance between energy intake and expenditure [45], the lean phenotype in PGKO mice is likely to be caused by decreased food intake as well as improved energy expenditure. In the current study, we found that deleting *GPSM1* in POMC neurons caused both hypophagia and increased thermogenesis. In contrast to the unaltered physical activities, increased thermogenic genes expression through SNS activation, was observed in PGKO mice under an HFD. All the effects may attribute to improved autophagy and leptin sensitivity of POMC neurons.

Leptin is mainly produced in the white adipose tissue and acts in different neuron cells, including POMC neurons, to regulate food intake and energy homeostasis [32]. To investigate whether the increased energy metabolism in PGKO mice was partly due to the improved leptin sensitivity, we detected food intake, p-STAT3 and c-FOS levels and calcium transients in POMC neurons after leptin treatment. Our results indicated that when *GPSM1* was deleted in POMC neurons, leptin sensitivity was obviously improved, preceding the induction of improved metabolic phenotypes. In POMC neurons, leptin activates both the STAT3 pathway to promote POMC mRNA expression and neuron axonal growth postnatally [46,47], and the transient receptor potential canonical (TRPC) channel to increase neuronal depolarization [48,49]. Correspondingly, we found POMC expression, α-MSH content and the activity of POMC neurons were all increased after depleting *GPSM1* from POMC neurons. Moreover, with the participation of leptin, activated melanocortin system improves the thermogenic function of BAT and evokes energy expenditure through increasing the distribution and activity of SNS [19], which means the increased thermogenesis and energy expenditure in PGKO mice in our study could be partly attributed to the improved leptin sensitivity.

Autophagy, an important intracellular mechanism that degrades damaged proteins and organelles, can interact with leptin signaling to achieve cellular homeostasis [50]. Interestingly, there have been evidence suggesting that GPSM1 could inhibit autophagy in a colorectal cancer mouse model and 293T cells [42,51]. Thus, we speculate that improved metabolic phenotypes in PGKO mice came from the enhanced autophagy in POMC neurons. As expected, we found *GPSM1* depleting in POMC neurons indeed promoted autophagy as decreased P62 and increased LC3BII protein levels *in vivo* and *in vitro*. Autophagy and leptin signaling could interact on each other in various cell types [36–38], here, we demonstrated that GPSM1 could regulate autophagy and leptin signaling in a cell-autonomous manner in POMC neurons. We further proved that the increased leptin sensitivity in PGKO mice was, at least, partly due to the regulation of GPSM1 on autophagy pathway. In view of the critical role of mTOR in energy metabolism and autophagy, here, we additionally revealed that the PI3K/AKT/mTOR pathway mediated the regulation of GPSM1 on autophagy in POMC cell lines. Moreover, as autophagy could increase the expression of POMC mRNA and POMC-derived α-MSH neuronal projections to PVN of the hypothalamus [35,52], our study also demonstrated that PGKO mice had increased POMC expression and α-MSH production. Therefore, we hold the opinion that in POMC neurons, GPSM1 could regulate energy intake and expenditure through influencing autophagy and leptin sensitivity, both of which could directly and/or indirectly be involved in the maintenance of appropriate POMC activity and α-MSH production.

There are several limitations in our study. Firstly, POMC is widely expressed in immature hypothalamus neurons, and in adult mice, half of embryonic POMC-expressing precursors subsequently adopt a non-POMC fate. Nearly one quarter of the mature NPY positive cell population shares a common progenitor with POMC positive cells. Thus, we could not exclude the potential contributions of altered POMC neuron development to the metabolic changes in the *GPSM1* depleted POMC progenitor cells. Tamoxifen-inducible *Pomc*-Cre mouse models are required to achieve adult-onset deletion. Secondly, we could not verify the precise mechanism through which GPSM1 regulates autophagy and leptin sensitivity in POMC neurons, as we had no POMC specific neuron cell line nor the technique to separate intact POMC neurons from mice. Although mHypoE-N43/5 cells are publicly considered as a POMC cell line, it comes from mouse embryonic hypothalamic tissue and consist of multiple types of neural populations. Further studies are still warranted to focus on the exact molecular mechanism of GPSM1 in POMC neurons for metabolic control involved. Finally, as *GPSM1* deletion in POMC neurons could protect from obesity and related metabolic deterioration, using a hybrid strategy combining computational and experimental approaches to look for the potential small-molecule compounds that interact with GPSM1 as well as counter its inhibitor effect on autophagy and leptin sensitivity might be a promising strategy. Further using the specific nano drug-delivery system to deliver the candidate small-molecule compounds to the POMC neurons through intranasal brain delivery might be expected to realize treating human obesity or metabolic disorders.

In summary, our results identify a new function of GPSM1 in hypothalamic POMC neurons in the regulation of energy homeostasis, obesity and obesity-related metabolic deterioration. Mechanistically, *GPSM1* deficiency in POMC neurons induced enhanced autophagy and improved leptin sensitivity through PI3K/AKT/mTOR signaling, thereby increasing POMC expression and α-MSH production, which ultimately increased thermogenesis in BAT via enhancing sympathetic innervation and activity. It also provides insights into a new potential therapeutic target for treating obesity and obesity-related metabolic diseases.

AUTHOR CONTRIBUTIONS

J.Y. and C.H. designed the study. M.T. carried out the experiments, analyzed the data, and wrote the manuscript. J.Y. helped to analyze the data and revised the manuscript. R.Z., Y.Z., J.Z., D.W. and X.W. assisted with the experiments. Y.Z. provided helpful suggestions about the experiments. J.Y. and C.H. directed the research.

ACKNOWLEDGEMENTS

This research was supported by grants from the National Science Foundation of China (81974118, 82370879, 82100908), the Shanghai Outstanding Academic Leaders (20XD1433300), the Shuguang Project (21SG11), Innovative research team of high-level local universities in Shanghai (SHSMU-ZDCX20212700), Major Natural Science Project of the Scientific Research and Innovation Plan of Shanghai Municipal Commission of Education (2023ZKZD17), Shanghai Research Center for Endocrine and Metabolic Diseases (2022ZZ01002), Shanghai Rising-Star Program (23QA1407400), Shanghai Sixth People's Hospital Affiliated to Shanghai Jiao Tong University School of Medicine (ynms202109), China Postdoctoral Science Foundation (2021M700088), and Shanghai Sixth People's Hospital Foundation (ynqn202106).

DECLARATION OF COMPETING INTEREST

The authors declare that they have no known competing financial interests or personal relationships that could have appeared to influence the work reported in this paper.

DATA AVAILABILITY

Data will be made available on request.

APPENDIX A. SUPPLEMENTARY DATA

Supplementary data to this article can be found online at https://doi.org/10.1016/j.molmet.2023.101839.

REFERENCES

[1] Haslam DW, James WP. Obesity. Lancet 2005;366(9492):1197—209.
[2] Piché ME, Tchernof A, Després JP. Obesity phenotypes, diabetes, and cardiovascular diseases. Circ Res 2020;126(11):1477—500.
[3] Lavie CJ, Alpert MA, Arena R, Mehra MR, Milani RV, Ventura HO. Impact of obesity and the obesity paradox on prevalence and prognosis in heart failure. JACC Heart Fail 2013;1(2):93—102.
[4] Câmara NO, Iseki K, Kramer H, Liu ZH, Sharma K. Kidney disease and obesity: epidemiology, mechanisms and treatment. Nat Rev Nephrol 2017;13(3):181—90.
[5] Fan JG, Kim SU, Wong VW. New trends on obesity and NAFLD in Asia. J Hepatol 2017;67(4):862—73.
[6] Bardou M, Barkun AN, Martel M. Obesity and colorectal cancer. Gut 2013;62(6):933—47.
[7] Iyengar NM, Gucalp A, Dannenberg AJ, Hudis CA. Obesity and cancer mechanisms: tumor microenvironment and inflammation. J Clin Oncol 2016;34(35):4270—6.
[8] Perdomo CM, Cohen RV, Sumithran P, Clément K, Frühbeck G. Contemporary medical, device, and surgical therapies for obesity in adults. Lancet 2023;401(10382):1116—30.
[9] Berthoud HR, Münzberg H, Morrison CD. Blaming the brain for obesity: integration of hedonic and homeostatic mechanisms. Gastroenterology 2017;152(7):1728—38.
[10] Gupta A, Osadchiy V, Mayer EA. Brain-gut-microbiome interactions in obesity and food addiction. Nat Rev Gastroenterol Hepatol 2020;17(11):655—72.
[11] Miller AA, Spencer SJ. Obesity and neuroinflammation: a pathway to cognitive impairment. Brain Behav Immun 2014;42:10—21.
[12] Ghamari-Langroudi M, Srisai D, Cone RD. Multinodal regulation of the arcuate/paraventricular nucleus circuit by leptin. Proc Natl Acad Sci U S A 2011;108(1):355—60.
[13] Idelevich A, Sato K, Nagano K, Rowe G, Gori F, Baron R. Neuronal hypothalamic regulation of body metabolism and bone density is galanin dependent. J Clin Invest 2018;128(6):2626—41.
[14] Jais A, Brüning JC. Arcuate nucleus-dependent regulation of metabolism-pathways to obesity and diabetes mellitus. Endocr Rev 2022;43(2):314—28.
[15] Bell BB, Harlan SM, Morgan DA, Guo DF, Cui H, Rahmouni K. Differential contribution of POMC and AgRP neurons to the regulation of regional autonomic nerve activity by leptin. Mol Metabol 2018;8:1—12.
[16] Vohra MS, Benchoula K, Serpell CJ, Hwa WE. AgRP/NPY and POMC neurons in the arcuate nucleus and their potential role in treatment of obesity. Eur J Pharmacol 2022;915:174611.
[17] Banno R, Zimmer D, De Jonghe BC, Atienza M, Rak K, Yang W, et al. PTP1B and SHP2 in POMC neurons reciprocally regulate energy balance in mice. J Clin Invest 2010;120(3):720—34.
[18] Tang Q, Liu Q, Li J, Yan J, Jing X, Zhang J, et al. MANF in POMC neurons promotes Brown adipose tissue thermogenesis and protects against diet-induced obesity. Diabetes 2022;71(11):2344—59.
[19] Williams KW, Liu T, Kong X, Fukuda M, Deng Y, Berglund ED, et al. Xbp1s in Pomc neurons connects ER stress with energy balance and glucose homeostasis. Cell Metabol 2014;20(3):471—82.
[20] Xiao Y, Deng Y, Yuan F, Xia T, Liu H, Li Z, et al. An ATF4-ATG5 signaling in hypothalamic POMC neurons regulates obesity. Autophagy 2017;13(6):1088—9.
[21] Taymans JM, Kia HK, Langlois X. Activator of G protein signaling type 3 mRNA is widely distributed in the rat brain and is particularly abundant in the subventricular zone-olfactory bulb system of neural precursor cell proliferation, migration and differentiation. Neurosci Lett 2006;391(3):116—21.
[22] Wang W, Li Q, Zou F, Yu Z, Wang Y, Lu T, et al. Increased expression of AGS3 in rat brain cortex after traumatic brain injury. J Neurosci Res 2013;91(5):726—36.
[23] Yip JLK, Lee MMK, Leung CCY, Tse MK, Cheung AST, Wong YH. AGS3 and Gα(i3) are concomitantly upregulated as part of the spindle orientation complex during differentiation of human neural progenitor cells. Molecules 2020;25(21).
[24] Bowers MS, McFarland K, Lake RW, Peterson YK, Lapish CC, Gregory ML, et al. Activator of G protein signaling 3: a gatekeeper of cocaine sensitization and drug seeking. Neuron 2004;42(2):269—81.
[25] Hofler C, Koelle MR. AGS-3 alters Caenorhabditis elegans behavior after food deprivation via RIC-8 activation of the neural G protein G αo. J Neurosci 2011;31(32):11553—62.
[26] Guo X, Zhang T, Shi L, Gong M, Jin J, Zhang Y, et al. The relationship between lipid phytochemicals, obesity and its related chronic diseases. Food Funct 2018;9(12):6048—62.
[27] Stunkard AJ, Blumenthal SA. Glucose tolerance and obesity. Metabolism 1972;21(7):599—602.
[28] Bartness TJ, Vaughan CH, Song CK. Sympathetic and sensory innervation of brown adipose tissue. Int J Obes 2010;34(1):S36—42. Suppl 1.
[29] Horie T, Nakao T, Miyasaka Y, Nishino T, Matsumura S, Nakazeki F, et al. microRNA-33 maintains adaptive thermogenesis via enhanced sympathetic nerve activity. Nat Commun 2021;12(1):843.
[30] Lim S, Honek J, Xue Y, Seki T, Cao Z, Andersson P, et al. Cold-induced activation of brown adipose tissue and adipose angiogenesis in mice. Nat Protoc 2012;7(3):606—15.
[31] Rosina M, Ceci V, Turchi R, Chuan L, Borcherding N, Sciarretta F, et al. Ejection of damaged mitochondria and their removal by macrophages ensure efficient thermogenesis in brown adipose tissue. Cell Metabol 2022;34(4):533—548.e12.
[32] Xu J, Bartolome CL, Low CS, Yi X, Chien CH, Wang P, et al. Genetic identification of leptin neural circuits in energy and glucose homeostases. Nature 2018;556(7702):505—9.
[33] Myers Jr MG, Leibel RL, Seeley RJ, Schwartz MW. Obesity and leptin resistance: distinguishing cause from effect. Trends Endocrinol Metabol 2010;21(11):643—51.
[34] Garcia-Marcos M, Ear J, Farquhar MG, Ghosh P. A GDI (AGS3) and a GEF (GIV) regulate autophagy by balancing G protein activity and growth factor signals. Mol Biol Cell 2011;22(5):673—86.
[35] Coupé B, Ishii Y, Dietrich MO, Komatsu M, Horvath TL, Bouret SG. Loss of autophagy in pro-opiomelanocortin neurons perturbs axon growth and causes metabolic dysregulation. Cell Metabol 2012;15(2):247—55.
[36] García-Miranda A, Solano-Alcalá KA, Montes-Alvarado JB, Rosas-Cruz A, Reyes-Leyva J, Navarro-Tito N, et al. Autophagy mediates leptin-induced migration and ERK activation in breast cancer cells. Front Cell Dev Biol 2021;9:644851.
[37] Huang ZM, Du SH, Huang LG, Li JH, Xiao L, Tong P. Leptin promotes apoptosis and inhibits autophagy of chondrocytes through upregulating lysyl oxidase-like 3 during osteoarthritis pathogenesis. Osteoarthritis Cartilage 2016;24(7):1246—53.

[38] Kamareddine L, Ghantous CM, Allouch S, Al-Ashmar SA, Anlar G, Kannan S, et al. Between inflammation and autophagy: the role of leptin-adiponectin Axis in cardiac remodeling. J Inflamm Res 2021;14:5349–65.
[39] Kaushik S, Arias E, Kwon H, Lopez NM, Athonvarangkul D, Sahu S, et al. Loss of autophagy in hypothalamic POMC neurons impairs lipolysis. EMBO Rep 2012;13(3):258–65.
[40] Malhotra R, Warne JP, Salas E, Xu AW, Debnath J. Loss of Atg12, but not Atg5, in pro-opiomelanocortin neurons exacerbates diet-induced obesity. Autophagy 2015;11(1):145–54.
[41] Heras-Sandoval D, Pérez-Rojas JM, Hernández-Damián J, Pedraza-Chaverri J. The role of PI3K/AKT/mTOR pathway in the modulation of autophagy and the clearance of protein aggregates in neurodegeneration. Cell Signal 2014;26(12):2694–701.
[42] Yang C, Yaolin S, Lu W, Wenwen R, Hailei S, Han Z, et al. G-protein signaling modulator 1 promotes colorectal cancer metastasis by PI3K/AKT/mTOR signaling and autophagy. Int J Biochem Cell Biol 2023;157:106388.
[43] Johnson PM, Kenny PJ. Dopamine D2 receptors in addiction-like reward dysfunction and compulsive eating in obese rats. Nat Neurosci 2010;13(5): 635–41.
[44] Lennerz B, Lennerz JK. Food addiction, high-Glycemic-index carbohydrates, and obesity. Clin Chem 2018;64(1):64–71.
[45] Wood PD. Impact of experimental manipulation of energy intake and expenditure on body composition. Crit Rev Food Sci Nutr 1993;33(4–5):369–73.
[46] Cowley MA, Smart JL, Rubinstein M, Cerdán MG, Diano S, Horvath TL, et al. Leptin activates anorexigenic POMC neurons through a neural network in the arcuate nucleus. Nature 2001;411(6836):480–4.
[47] Santoro A, Campolo M, Liu C, Sesaki H, Meli R, Liu ZW, et al. DRP1 suppresses leptin and glucose sensing of POMC neurons. Cell Metabol 2017;25(3):647–60.
[48] Gao Y, Yao T, Deng Z, Sohn JW, Sun J, Huang Y, et al. TrpC5 mediates acute leptin and serotonin effects via Pomc neurons. Cell Rep 2017;18(3):583–92.
[49] Qiu J, Wagner EJ, Rønnekleiv OK, Kelly MJ. Insulin and leptin excite anorexigenic pro-opiomelanocortin neurones via activation of TRPC5 channels. J Neuroendocrinol 2018;30(2).
[50] Mizushima N, Komatsu M. Autophagy: renovation of cells and tissues. Cell 2011;147(4):728–41.
[51] Groves B, Abrahamsen H, Clingan H, Frantz M, Mavor L, Bailey J, et al. An inhibitory role of the G-protein regulator AGS3 in mTOR-dependent macroautophagy. PLoS One 2010;5(1):e8877.
[52] Cao C, Gao T, Cheng Y, Cheng M, Su T, Xi F, et al. Hypothalamic AMPK-induced autophagy ameliorates hypercatabolism in septic rats by regulating POMC expression. Biochem Biophys Res Commun 2018;497(4):1089–96.

